Steady-State, Applied-Field, Rectangular MPD Thrusters

IEPC-2013-246

Presented at the 33rd International Electric Propulsion Conference,
The George Washington University • Washington, D.C. • USA
October 6 – 10, 2013

Shigeru Yokota[1], Daisuke Ichihara[2], Hisashi Kataoka[2], Shota Harada[2] and Akihiro Sasoh[3]
Nagoya University, Nagoya, Aichi, 464-8603, Japan

Abstract: A steady state, applied field, rectangular magnetoplasmadynamic (MPD) thruster with permanent magnets has been developed. To evaluate the thrust performance, thrust and discharge voltage were measured varying propellant mass flow rate, discharge current and inter-electrode distance. Analyzing the result, it was declared that smaller mass flow rate enhances the thrust efficiency. To realize these conditions, argon/hydrogen mixture propellant was used. As a result, the thrust efficiency reaches to 27% at 9100 sec of specific impulse was obtained.

Nomenclature

B	=	applied magnetic field
$\mathbf{B}$	=	magnetic field (vector)
e	=	elementary electric charge
F	=	thrust
g	=	gravitational constant
H	=	inter-electrode distance
I_{sp}	=	specific impulse
J_d	=	discharge current
J_k	=	keeper current
$\mathbf{j}$	=	discharge current density
$\dot{m}_1$	=	mass flow rate through the hollow cathode
$\dot{m}_2$	=	mass flow rate through the discharge channel back plate
n_e	=	electron number density
p_e	=	electron pressure
u_{ex}	=	exhaust velocity
$\bar{u}$	=	representative value of flow velocity
V_d	=	discharge voltage
V_k	=	keeper voltage
V_{sheath}	=	effective sheath voltage
η	=	thrust efficiency
σ	=	electric conductivity

I. Introduction

A steady state, magnetoplasmadynamic (MPD) thruster is one of the most promising electric propulsion (EP) systems for an orbit transfer vehicle or a deep space probe because of its higher thrust density and specific

[1] Assistant Professor, Department of Aerospace Engineering, yokota@nuae.nagoya-u.ac.jp.
[2] Student, Department of Aerospace Engineering.
[3] Professor, Department of Aerospace Engineering, sasoh@nuae.nagoya-u.ac.jp.

impulse (Isp) than other EP systems [1, 2]. Also, the MPD thruster has several other advantages: a structural simplicity, high flexibility in propellant species, variable Isp, and so on. However the MPD thruster has never been loaded on a satellite in practical use because of its lower thrust efficiency, difficulty of ignition, and shorter lifetime than other EP system such as ion engines or Hall thrusters.

In order to solve these problems, comprehension of the energy balance in the thruster is important, so that we have developed an applied field (AF) type MPD thruster. The thruster has a gas fed type hollow cathode for easy ignition and longer lifetime. The thruster has a rectangular acceleration channel. Indeed most of conventional AF-MPD thrusters have coaxial discharge channels, which are consisted of central cathode rods and axisymmetric anodes [3-5], however recent researches in ISAS/JAXA discovered gradually that a rectangular type MPD thruster has a good performance [6, 7]. Also, the rectangular type thruster is easy to realize the phenomena inside the thruster.

In this paper, the thrust performance of the MPD thruster we developed is reported and discussed.

II. Experimental setup

A. MPD thruster head

The schematic of the MPD thruster is illustrated in Fig. 1. The rectangular discharge channel width and length are 20 mm and 60 mm, respectively. The inter-electrode distance, H, is varied from 5 to 15 mm. The upper wall is anode made of molybdenum which divided into five pieces to measure discharge current distribution. On the lower wall, a hollow cathode (DLHC-1000, Kaufman & Robinson Inc.) was mounted. The propellant (Argon) was fed to the discharge channel through hollow cathode. An external magnetic field was applied to the discharge channel by two neodymium magnets connected with an iron yoke. The magnetic flux density was 240 mT at the center of the discharge channel (Fig. 2).

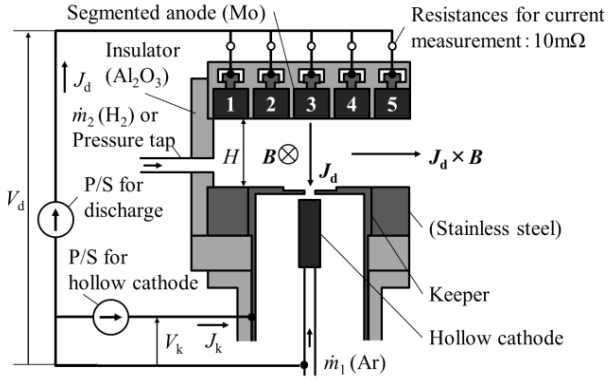

Figure 1. Schematic of the MPD thruster head.

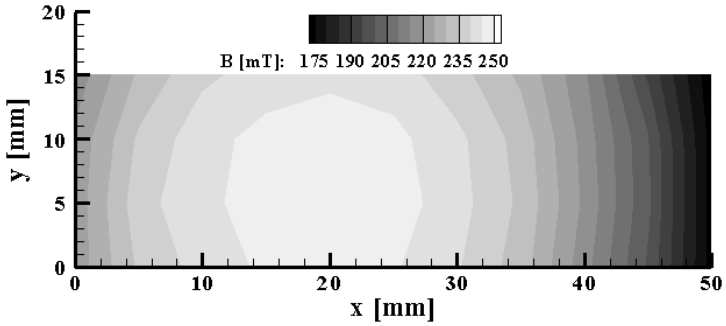

Figure 2. Amplitude of magnetic flux density distribution in the discharge channel

B. Vacuum system and measurement system

The experiments in this study were conducted in a vacuum chamber whose diameter and length are 2 m and 4m respectively (Figure 3). The vacuum chamber is evacuated using a turbo molecular pump (3200L/s) backed by a rotary pump (33.3L/s). The ambient pressure in the vacuum chamber was measured by an ionization vacuum gauge

and a pirani gauge. The ambient pressure without propellant flow was 10^{-3} Pa; at the mass flow rate of 1.25 mg/s, ambient pressure was 5.5×10^{-2} Pa.

Thrust was measured using a pendulum type thrust stand. It consists of a stand arm, a vacuum bellows and two radial bearings. A differential transformer is used to detect the pendulum oscillation amplitude. Thrust, discharge voltage and keeper voltage were measured varying propellant mass flow rate, discharge current and inter-electrode distance. These data were logged using cDAQ-9178 (National Instruments).

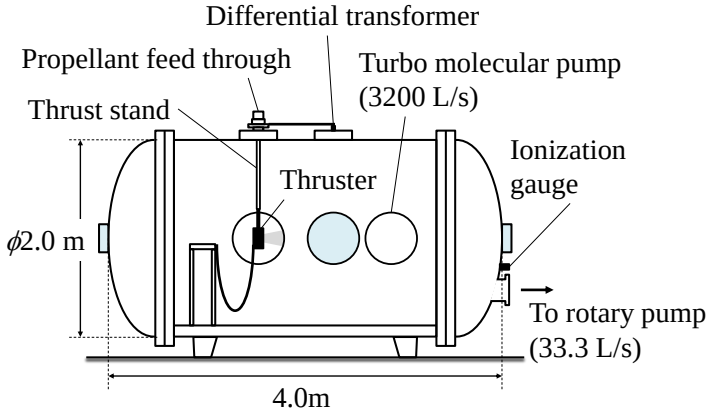

Figure 3. Experimental setup

III. Mono-propellant operation

A. Operation condition

The operation condition is tabulated on Table 1. The propellant was fed only through the hollow cathode.

Table 1Operation condition

Control parameter	Symbol		Value
Mass flow rate from hollow cathode [mg/s]	$\dot{m}_1$	Ar	0.41, 0.83, 1.25
Mass flow rate from back plate [mg/s]	$\dot{m}_2$		0
Discharge current [A]	J_d		5, 10, 15
Keeper current [A]	J_k		2
Applied magnetic field [mT]	B		240
Inter-electrode distance [mm]	H		5, 10, 15

B. Operation characteristics

Dependency on $\dot{m}$

Figure 4 shows F as a function of $\dot{m}$. As shown in this figure, F was almost independent on $\dot{m}$. This tendency indicates that the electromagnetic acceleration is dominant in this operation region. The pressure thrust, which was estimated by the pressure on the channel back plate, was less than 11% of the total thrust.

Figure 5 shows V_d and back electromagnetic force (EMF) $\overline{u}BH$ as a function of $\dot{m}$. Both V_d and $\overline{u}BH$ decreased as decreasing of $\dot{m}$. This V_d decrement must be caused by the decrement of the back EMF.

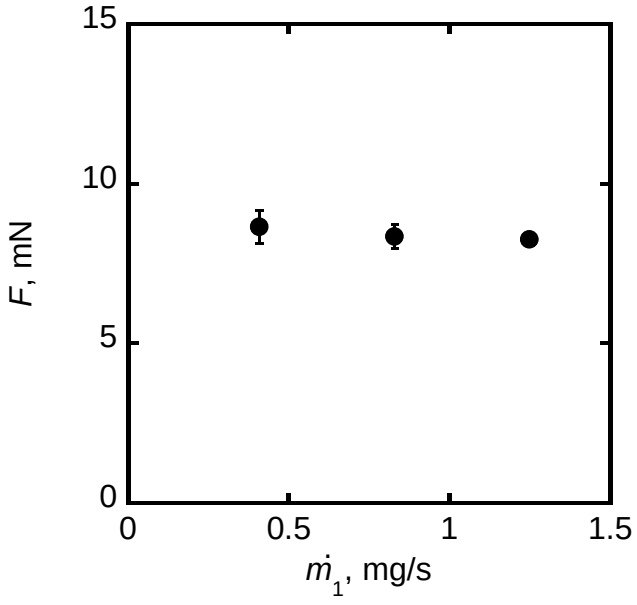

Figure 4 F as a function of $\dot{m}_1$. *Jd=10 A, B=240 mT, H=10 mm.*

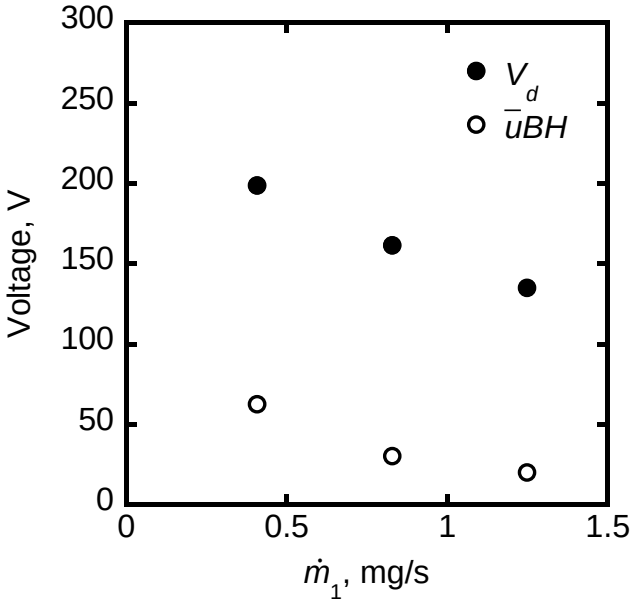

Figure 5 V_d and $\overline{u}BH$ as a function of $\dot{m}_1$. *J_d=10 A, B=240 mT, H=10 mm.*

Thrust performance

Ideally, F should be proportional to the Lorentz force J_dBH when the electromagnetic acceleration is dominant. Figure 6 shows the F as a function of J_dBH. The measured thrust is smaller than the ideal Lorentz force.

In order to identify the cause of the loss, F vs. J_d and H are checked independently. Figure 7 shows F as a function of J_d. As shown in this figure, F is almost proportional to J_d. On the other hand, figure 8 shows F as a function of H. As shown in this figure, F/J_dBH increases as H increases. According to the square-cubic law, the loss is assumed to be caused by the accelerated particle loss to the wall.

To verify this assumption, we measured the discharge current distribution in the discharge channel. Figure 9 shows the current distribution on the anode. As shown in this figure, 70% of discharge current flows through the middle anode. This result implies that the charged particles are accelerated in the middle of the discharge channel then a part of them go to the wall or the electrodes.

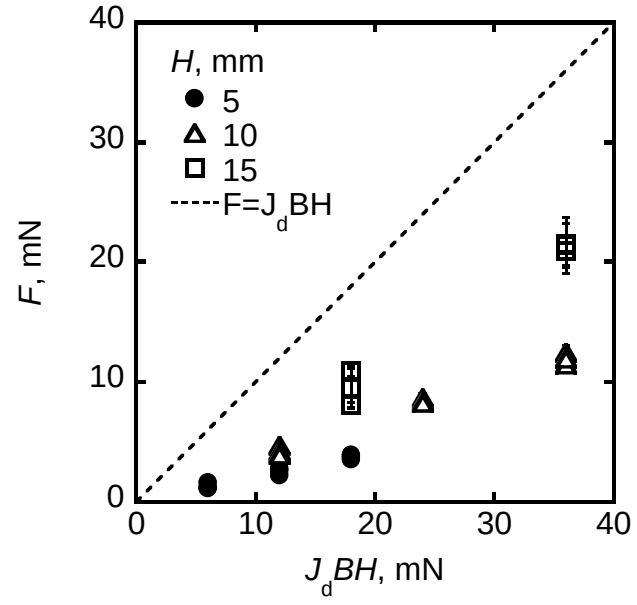

Figure 6 F as a function of J_dBH. *$\dot{m}_1$=0.41-1.25, J_d=5-15A, B=240 mT.*

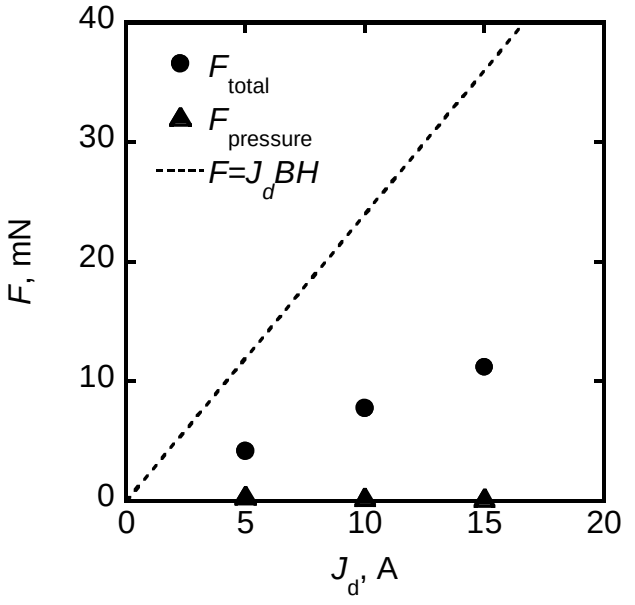

Figure 7 V_d as a function of J_d. *$\dot{m}_1$=1.25 mg/s, B=240 mT, H=10 mm.*

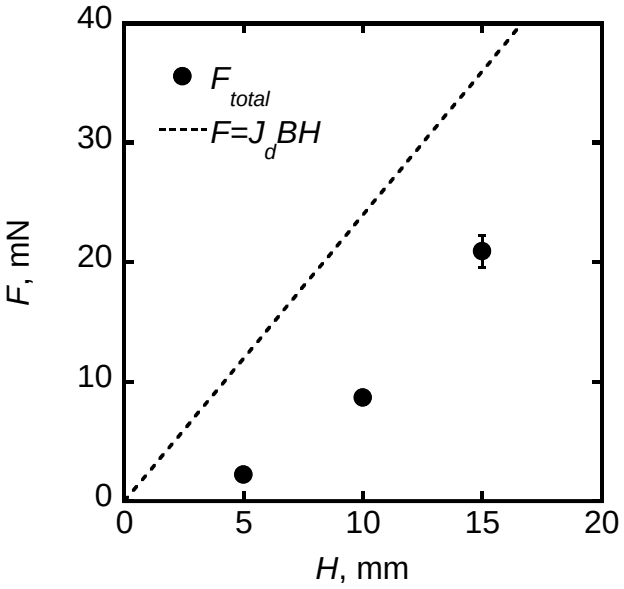

Figure 8 *F* as a function of *H*, $\dot{m}_1$*=0.41 mg/s, B=240 mT, H=10 mm.*

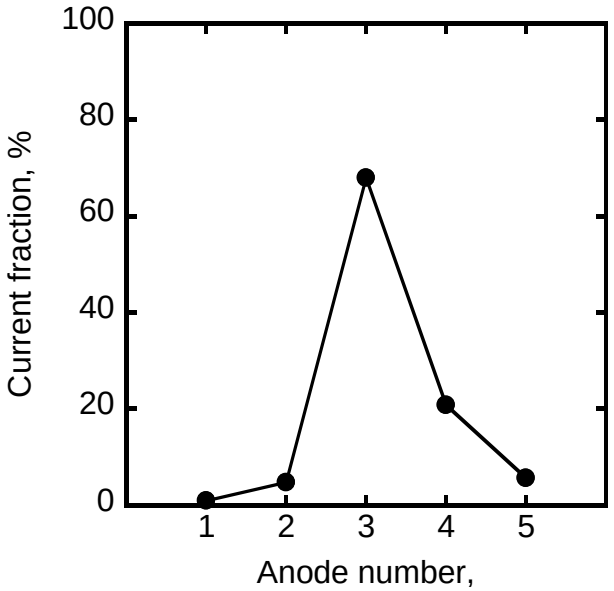

Figure 9 Discharge current distribution, $\dot{m}_1$*=0.41mg/s, J_d=5A, B=240 mT, H=10 mm.*

Discharge voltage characteristics

Assuming the plasma in the thruster is fully ionized, generalized Ohm's law is

$$\mathbf{j} = \sigma\left(\mathbf{E} + \mathbf{u}\times\mathbf{B} - \frac{1}{en_\mathrm{e}}\mathbf{j}\times\mathbf{B} + \frac{1}{en_\mathrm{e}}\nabla p_\mathrm{e}\right) \tag{1}$$

After solving for E in Eq. (1), integrating along a current path through the plasma from anode to cathode, and adding sheath voltage, discharge voltage is given by,

$$\begin{aligned} V_\mathrm{d} &= \int_{\text{Anode}}^{\text{Cathode}} \mathbf{E}\cdot d\mathbf{s} + V_\mathrm{sheath} = \left(\bar{u}B + \frac{J_\mathrm{d}}{\bar{\sigma}WL} - \frac{\nabla p_\mathrm{e}}{en_\mathrm{e}}\right)H + V_\mathrm{sheath} = \beta H + V_\mathrm{sheath} \\ \beta &\equiv \beta_1 + \beta_2, \quad \beta_1 = \bar{u}B = \frac{u_\mathrm{ex}B}{2} = \frac{J_\mathrm{d}B^2H}{2\dot{m}}, \quad \beta_2 = \frac{J_\mathrm{d}}{\bar{\sigma}WL} - \overline{\left(\frac{\nabla p_\mathrm{e}}{en_\mathrm{e}}\right)} \end{aligned} \tag{2}$$

here, V_sheath is sum of the anode sheath voltage and the cathode sheath voltage. The first term $\bar{u}BH$, is back EMF and the other terms express thermoelectric power.

Figure 9 shows an example of voltage equivalent energy balance. Assuming that β is constant in any inter-electrode distance case under the condition of constant $\dot{m}/H$, V_sheath is obtained as the ordinate intercept because it is not a function of *H*. The estimated sheath voltage is about 25 V, which is 10 % of the total voltage. On the other hand, the back EMF is about 15 % of the total power in this case.

To improve the energy efficiency, the discharge voltage except for the sheath voltage should be high enough to ignore sheath voltage. For example, the low propellant flow rate operation is desirable because $\bar{u}BH$ increases as $\dot{m}_1$ decreases (Fig. 5).

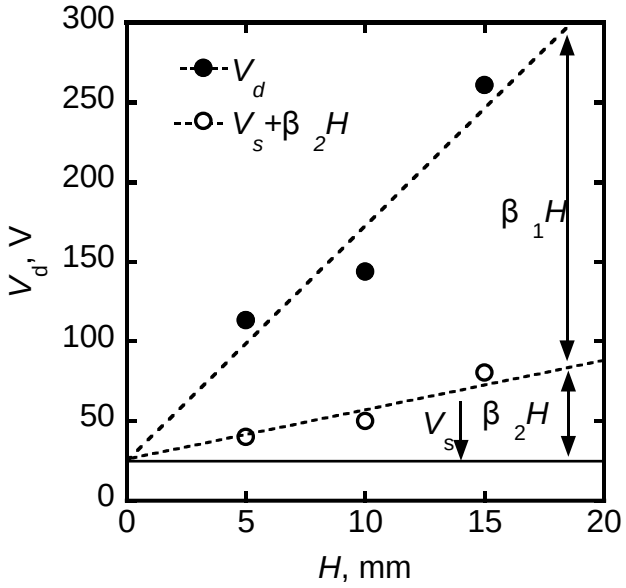

Figure 9. Estimate sheath voltage, *J_d=10 A, B=240 mT, $\dot{m}_1/H$=0.041 mg/(s ·mm)*

IV. Bi-propellant operation

As mentioned above, the thrust efficiency is enhanced by the lower mass flow rate. To satisfy the condition, hydrogen was used as a propellant. Using hydrogen, mass flow rate becomes smaller because of the smaller molecular mass of hydrogen than that of argon. In this study, we mixed argon and hydrogen to operate the thruster because argon was needed to operate the hollow cathode. The hydrogen fed through the back plate of the discharge channel (See Figure 1). The volume flow rate of hydrogen to that of argon was 1:1.

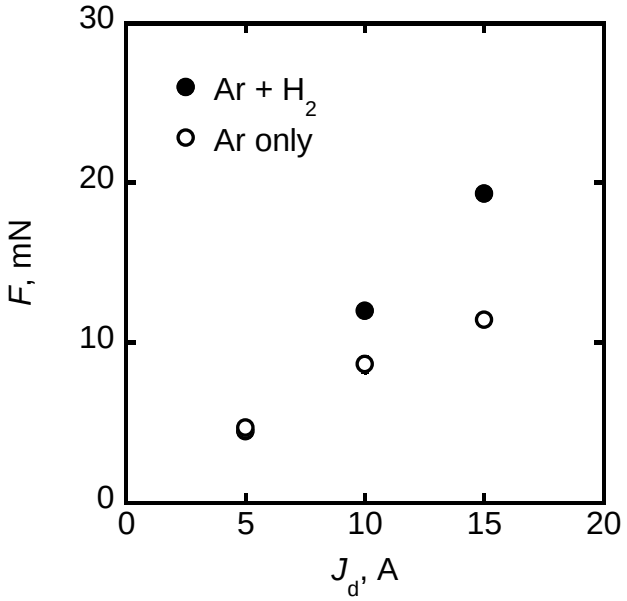

Figure 10 ***F*** **as a function of** ***J_d***, *Total mass flow rate=10sccm, $\dot{m}_1$=0.2 mg/s (5 sccm), $\dot{m}_2$=0.01 sccm (5 sccm), B=240mT, H=10 mm*

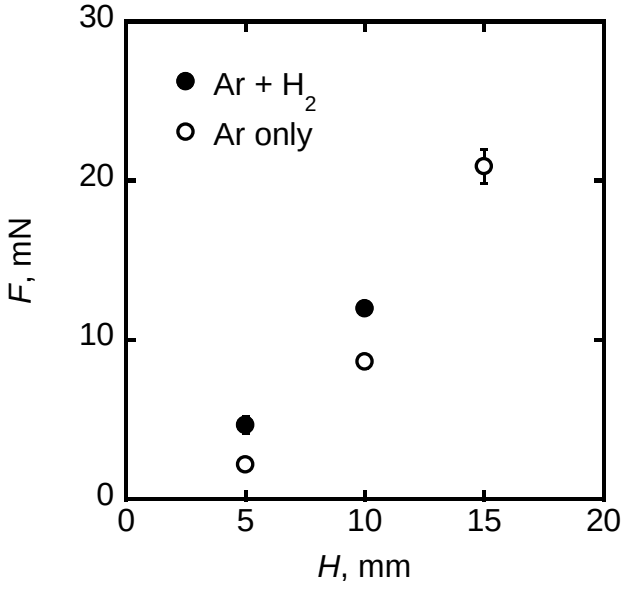

Figure 11 ***F*** **as a function of** ***H***, *Total mass flow rate=10sccm, $\dot{m}_1$=0.2 mg/s (5 sccm), $\dot{m}_2$=0.01 sccm (5 sccm), B=240 mT, H=10 mm*

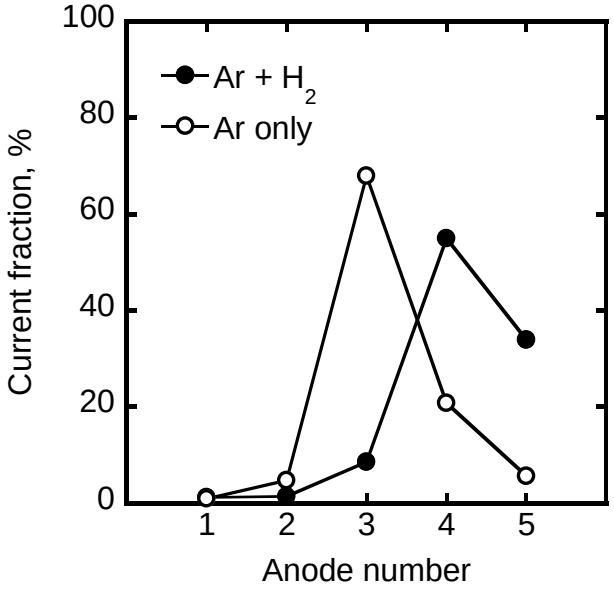

Figure 12 Discharge current distribution under bipropellant operation, *total mass flow rate=10 sccm, $\dot{m}_1$=5 sccm, $\dot{m}_2$=5 sccm, J_d=5A, B=240 mT*

Figures 10 and 11 show measured F varying J_d and H, respectively. As shown in these figures, F in the case of Ar-H_2 mixture gas was larger than that in the Ar only case. The discharge current distribution also measured (Fig. 13). By adding hydrogen, discharge current distributed downstream region of discharge channel, 75% of discharge current distributed in the downstream region in the discharge channel (anode #4 and #5). This result indicates that the ionized propellant was exhausted before interacting with discharge channel wall and thrust increased.
The lower mass flow rate and the higher thrust means higher $\overline{u}BH$, while the total discharge voltage did not changed by adding H_2 (Figures 13 and 14). The other terms in equation (2) must be decreased, however, the fraction has not been declared yet.

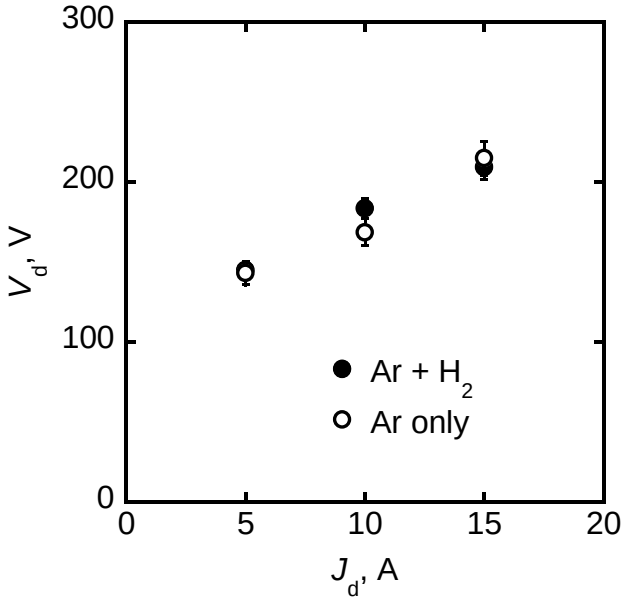

Figure 13 V_d as a function of J_d, *Total mass flow rate=10sccm, $\dot{m}_1$=0.2 mg/s (5 sccm), $\dot{m}_2$=0.01 sccm (5 sccm), B=240mT, H=10 mm*

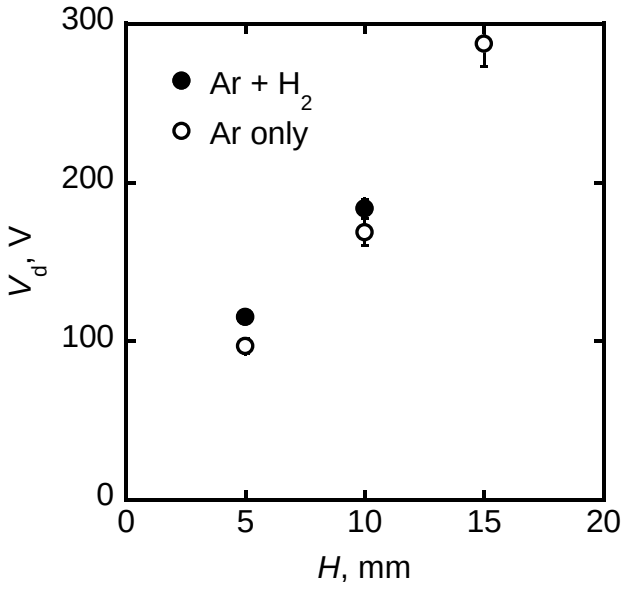

Figure 14 V_d as a function of H, *Total mass flow rate=10sccm, $\dot{m}_1$=0.2 mg/s (5 sccm), $\dot{m}_2$=0.01 sccm (5 sccm), B=240 mT, H=10 mm*

V. Thrust performance

The thrust efficiency can be divided into two parts; one is the measured thrust to ideal electromagnetic force ratio; the other is back EMF to total discharge voltage ratio.

$$\eta = \frac{F^2}{2\dot{m}J_d V_d} = \frac{\bar{u}BH}{V_d} \cdot \frac{F}{J_d BH}, \quad \bar{u} = \frac{u_{ex}}{2} \tag{3}$$

Adding H_2 contributes to both higher $\bar{u}BH/V_d$ and F/J_dBH.

Thruster performance is summarized in Fig. 15. By adding hydrogen, specific impulse and thrust efficiency increased because propellant mass flow rate became lighter and thrust increased. Under the bi-propelllant operating condition, the maximum thrust efficiency was 27% at specific impulse was 9100 sec.

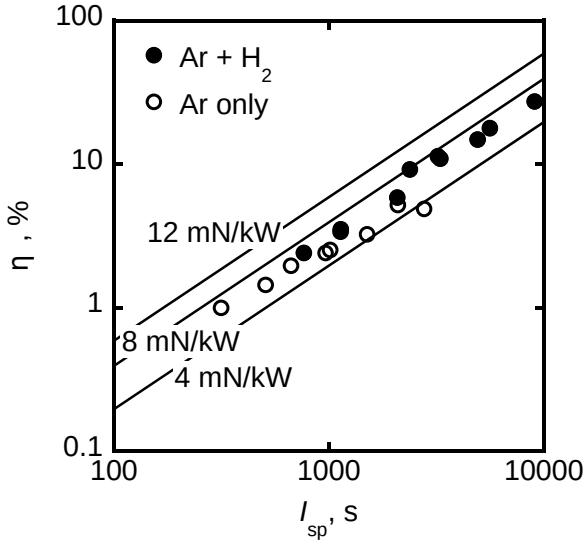

Figure 15 Thruster performance, *total mass flow rate=10-30sccm, $\dot{m}_1$=5-15 sccm, $\dot{m}_2$=5-15 sccm, J_d=5-15A, B=240 mT, H=10mm.*

Conclusion

An experimental study of a steady state, applied field, rectangular MPD thruster has been performed. As a result, it is declared that the thrust efficiency is enhanced by the lower mass flow rate. In order to realize the condition, argon/hydrogen mixture gas was used as a propellant. Adding hydrogen improves not only the back EMF to the total discharge voltage ratio but also the thrust to the ideal electromagnetic force. As a result, maximum thrust efficiency was improved and reached to 27% at specific impulse was 9100 sec.

References

[1]M. Auwetwe-Kurtz et al. "Optimization of Electric Thrusters for Primary Propulsion Based on the Rocket Equation," IEPC01-181.

[2]K. Toki et al. "Application of MPD Thruster System to Interplanetary Missions," AIAA Paper-85-2026.

[3]E. Choueiri "On the Thrust of Self-Field MPD Thrusters," IEPC Paper 97-121.

[4]G. Krulle et al. "Technology and Application Aspects of Applied Field Magnetoplasmadynamic Propulsion," Journal of Propulsion and Power, 14, 5 (2009) pp. 754-763.

[5]M. Auwetwe-Kurtz et al. "Plasma Thruster Development Program at the IRS," Acta Astronautica, 32, 5 (1994) pp. 377-391.

[6]K. Toki et al, "Multi Channel Two Dimensional MPD Arcjet", Journal of Propulsion and Power," Vol. 8, No. 1, pp. 93.

[7]A. Iwakawa et al. "Performance or Two-Dimensional Applied-Field Magneto – Plasma – Dynamic Thruster," IEPC Paper 2009-226.

[8]M. Takubo, et al. "The Relation between Crossed Applied Magnetic Field MPD Thruster Electrode Shapes and Thrust, and Plasma Emission," STEP-2011-025 (in Japanese).